# The Numerical Solution of Some Important Transmission-Line Problems

## HARRY E. GREEN

*Abstract*—The generalized numerical solution of Laplace's equation in two dimensions is dealt with, subject to boundary conditions imposed by conducting surfaces and dielectrics which are permitted a limited amount of inhomogeneity. It is shown how this solution may be applied in the determination of the properties of TEM-mode transmission lines including the equivalent circuits of simple obstacles in these lines. The theory is illustrated with a number of examples, certain of which do not appear to have been previously treated theoretically in the literature. While certain of the examples serve mainly to show the power of the technique, others are given very detailed treatment with the production of much new design data.

## I. INTRODUCTION

TWO IMPORTANT CLASSES of problems in transmission-line engineering, each requiring the solution of Laplace's equation, will be treated. The aims of the paper are:

1) To outline these problems,
2) To present the mathematical theory for their numerical analysis,
3) To summarize the numerical analysis procedures and their use in constructing a computer program
4) To give an extensive collection of important engineering results that have been obtained.

The first class of problem is concerned with the determination of the characteristic impedance and propagation constant of TEM-mode transmission lines. For engineering exploitation an accurate knowledge of the basic parameters of these lines is necessary. Because the mode is TEM, having components of neither the electrical nor the magnetic fields in the direction of propagation, the determination of these constants requires a study of the fields only over the line cross section, within which they must obey Laplace's equation and the imposed boundary conditions.

The second type of problem considers the outcome when the longitudinal uniformity of a TEM mode line is interrupted by the insertion of an obstacle. The regions of inhomogeneous field so generated can often be represented by equivalent circuits referred to suitably chosen reference planes enclosing the obstacle. In certain special but important cases, the parameters of these equivalent circuits can be found by solution of the Laplace equation within the inhomogeneous region.

Despite the success of modern analysis there remain many problems of engineering importance of both types which either were left unsolved or were treated approximately and with varying success. This is particularly true where not only do the boundary conditions imposed by the conductors have to be taken into account but also, additional constraints are imposed by the presence of an inhomogeneous dielectric medium. The numerical techniques that form the subject of this paper must then be employed.

## II. THEORY

### A. Numerical Analysis Theory

It must be made clear from the outset that this work is concerned exclusively with two-dimensional systems whose boundaries can be represented as a series of constant coordinate curves in either

1) Cartesian coordinates, or
2) cylindrical coordinates, with the restriction of rotational symmetry

In each case a special kind of inhomogeneity in the dielectric medium will be permitted. That is, two dielectrics may be present, one of which is free space, and the whole dielectric is considered to be made up by the juxtaposition of discrete blocks of these dielectrics, i.e., the inhomogeneities are stepwise. "Dielectric," will be defined, hereafter, to mean the nonfree space portion.

Cartesian problems require the solution of the equation

$$\frac{\partial^2 V}{\partial x^2} + \frac{\partial^2 V}{\partial y^2} = 0 \tag{1}$$

while in cylindrical coordinates the following equation must be solved:

$$\frac{\partial^2 V}{\partial r^2} + \frac{1}{r}\frac{\partial V}{\partial r} + \frac{\partial^2 V}{\partial z^2} = 0. \tag{2}$$

The numerical solutions of both these equations have much in common and it will suffice here to develop the argument for the Cartesian case only. The treatment of cylindrical problems is given in Appendix A.

Consider the two-dimensional problem shown in Fig. 1. For the present, some generality may be sacrificed without essential loss to the outline of the theory by considering the medium between the conductors to be homogeneous. Details of the treatment of inhomogeneous media appear in Appendix B. Imagine the region
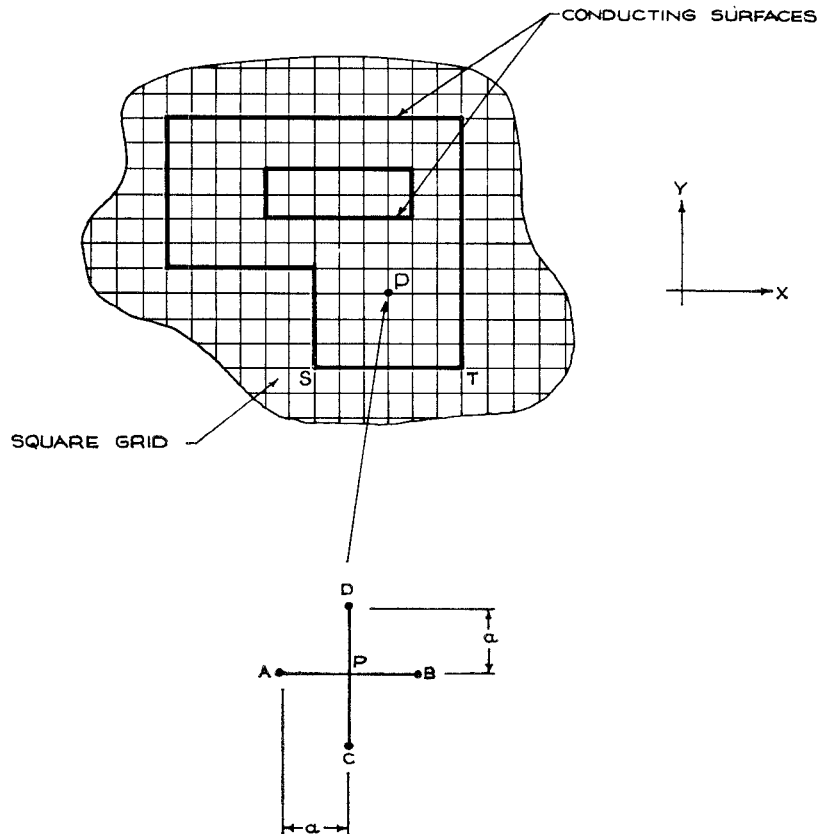
Fig. 1.  Basic finite difference net.

between the conductors to be divided into squares by a net of interlaced rows and columns. Although the figure shows the conductors falling along these rows and columns this is not an essential element in the theory. However, for the purpose of organizing the problem on a computing machine it is much easier if this is the case; this restriction has been voluntarily imposed throughout this work.

Consider a typical point $P$ in the medium between the conductors. The potential at $P$ must satisfy (1). For numerical computation, this equation can be reduced by considering it in terms of the potential at $P$ and its four immediate neighbors, distant by the mesh width $a$ in each of the coordinate directions. Then applying Taylor's theorem in the $X$ direction.

$$V_B - V_P = a\frac{\partial V}{\partial x} + \frac{a^2}{2!}\frac{\partial^2 V}{\partial x^2} + \frac{a^3}{3!}\frac{\partial^3 V}{\partial x^3} + \frac{a^4}{4!}\frac{\partial^4 V}{\partial x^4} +$$

$$V_A - V_p = -a\frac{\partial V}{\partial x} + \frac{a^2}{2!}\frac{\partial^2 V}{\partial x^2} - \frac{a^3}{3!}\frac{\partial^3 V}{\partial x^3} + \frac{a^4}{4!}\frac{\partial^4 V}{\partial x^4} -,$$

adding, and then manipulating.

$$\frac{\partial^2 V}{\partial x^2} = \frac{V_A + V_B - 2V_P}{a^2} - \frac{a^2}{12}\frac{\partial^4 V}{\partial x^4} -$$

$$\simeq \frac{V_A + V_B - 2V_P}{a^2}, \tag{3}$$

i.e., an approximation has been obtained to the second derivative, accurate within the order $a^2$, and which can be arbitrarily refined by decreasing the mesh width.

The same argument may be applied in the $Y$ direction. Combining this with (3), (1) for $P$ reduces to

$$V_A + V_B + V_C + V_D - 4V_P = 0 \tag{4}$$

and this may be extended to every other point in the medium. For nodes on the conducting boundaries by definition

$$V_P = V_0 \tag{5}$$

where $V_0$ is the boundary potential.

The original problem, therefore, was replaced by one which gives an approximate representation in terms of simultaneous linear equations, i.e., a complex analytic problem was reduced to solving simultaneous equations.

B. The Solution of Large Groups of Simultaneous Equations

Although the problem undoubtedly has been simplified it is not all gain since an adequate representation of the original problem demands a large group of simultaneous equations which need special techniques for solution, i.e., the basic problem now is one of coping with the large amount of arithmetic involved.

Solution by digital computer has been receiving much attention during the last ten years and is now the subject of a large and increasing volume of literature [1].

Of the many possible processes for the solution of the simultaneous equations arising in the finite difference treatment of partial differential equations, the one which seems best suited to a digital machine is successive over-relaxation (SOR). This has the advantages of

1) involving only the constant repetition of a small group of machine orders,
2) allowing the data relating to substantially large problems to be retained entirely in core, and
3) being terminable when any desired degree of accuracy has been attained. This is important since it is fruitless to solve what is, after all, only an approximation to the actual problem to an accuracy greater than that of the approximation.

SOR may be defined as the relaxation cycle [2],

$$V_{i(j+1)} = V_{i(j)} - \frac{\Omega}{a_{ii}} \left\{ \sum_{k=1}^{n} a_{ik} V_{k(j)} - b_i \right\}, \qquad (6)$$

whereby a gradually improving solution is obtained to the simultaneous equations written in matrix form as

$$A V = B$$

where

$a_{ik}$, $V_i$, $b_i$ are elements of the matrices $A$, $V$, $B$, respectively,
$j$ measures the number of iteration cycles,
$n$ is the number of simultaneous equations, and
$\Omega$ is the accelerating factor.

The method is convergent if $0 < \Omega < 2$, and most rapidly convergent for some $\Omega_0$ between 1 and 2.

For efficient computation the crux of the problem is to determine the optimum accelerating factor $\Omega_0$. Frankel [3] showed that this is dependent upon the largest eigenvalue of a certain matrix derived from $A$ and itself dependent on $\Omega_0$. In general, then, except in the most trivial cases, it is just as difficult to solve for $\Omega_0$ as to do the actual problem, and it is generally not possible to start the computation with a knowledge of this parameter.

This difficulty was overcome by Carré [4] who devised a method of determining $\Omega_0$ with steadily improving accuracy as the calculation proceeds.[1] While obviously not as fast as optimum SOR, it still saves considerable time when compared with other possible methods. Carré's paper is also important in that in it he gives a method for estimating an upper bound on the largest remaining error after any complete iteration cycle. This may be used as a terminating criterion.

[1] In the solution of a few cylindrical coordinate problems, some difficulty has been experienced by early estimates of accelerating factor being greater than two. The difficulty was overcome by setting a ceiling value of 1.95 on this factor. This early instability soon disappears and a close approximation to the optimum $\Omega_0$ is ultimately found. An explanation of this anomalous behavior is given in [5].

## C. Determination of Transmission-Line Constants

The way is open to compute the constants of transmission lines if a nodal potential distribution is known. Capacity is the first constant sought and for some purposes, e.g., equivalent circuits of discontinuities, this is also the final result.

To obtain capacity it is prerequisite to determine the charges on the conductors. These may be found by Gauss theorem [6], requiring the integration of the normal component of electric displacement over a surface enclosing the conductor. Forming this surface by lines joining nodal points drawn parallel to the coordinate directions, as shown in Fig. 2, at any point $P$ on this surface

$$D_n = \epsilon E_n = -\epsilon \frac{\partial V}{\partial n}, \qquad (7)$$

where

$D_n$ is the normal component of displacement,
$E_n$ is the normal component of electric intensity, and
$n$ is the normal coordinate.

By the same Taylor expansion as used earlier the derivative of the potential at $P$ may be expressed numerically in terms of the known potentials of the nodes $A$ and $B$ on each side of it, with an error in the order of $a^2$, as

$$\frac{\partial V}{\partial n} = \frac{V_B - V_A}{2a}. \qquad (8)$$

It is now easy to apply Gauss' theorem. Thus, if the surface containing the conductor consists of $s$ straight line segments each containing $r$ nodes, the charge per unit length normal to the cross-section is given by

$$Q = \epsilon a \sum_{s} \sum_{P=1}^{r} \left( \frac{\partial V}{\partial n} \right)_P \qquad (9)$$

where the symbol $\sum'$ is used to indicate that the first and last terms in the summation are halved. This is seen to be equivalent to integration by the trapezoidal rule, known to involve a dominant error in the order $a^2$, and is therefore consistent with the whole finite difference process.

From charge capacity it follows that

$$C = Q V_t^{-1} \qquad (10)$$

where $V_t$ is the potential difference between the conductors. Given capacity, characteristic impedance follows without difficulty, although two cases need to be distinguished. If the medium within the line is homogeneous,
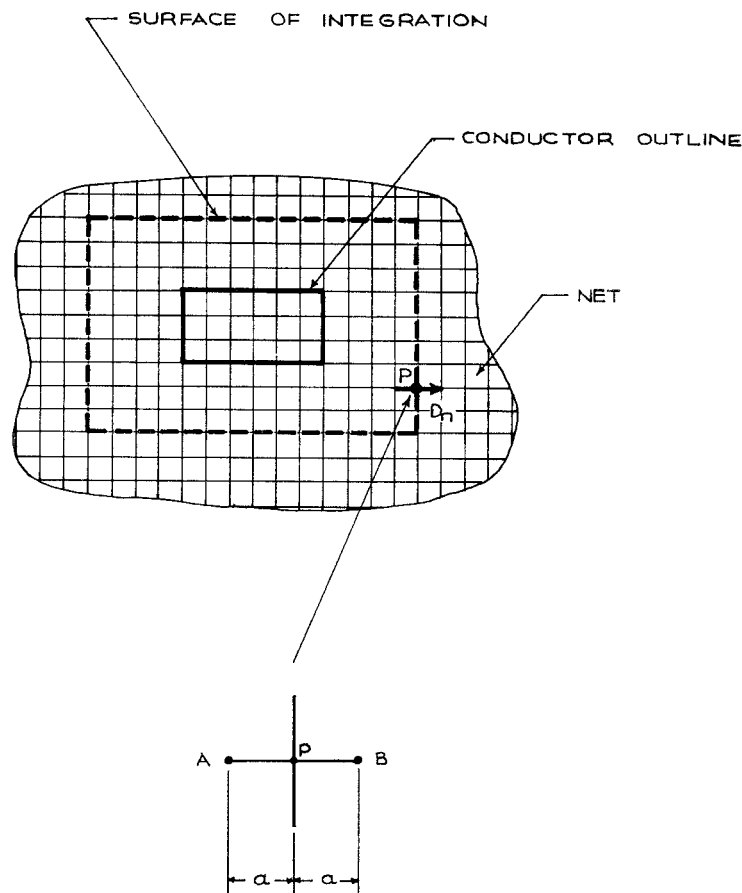
$$Z_0 = \frac{1}{Cv} \qquad (11)$$

Fig. 2.   Integration to determine charge.

where

$v = v_0 / \sqrt{K_e}$ is the phase velocity in the medium
$v_0$ = the velocity of light in free space
    $(2.997925 \times 10^8$ m/s$)$, and
$K_e$ = the dielectric constant of the medium.

If the medium is inhomogeneous, two steps are necessary: the capacity is determined twice, once with all dielectrics removed, and then with them present. Since inductance per unit length is not altered by the introduction of the dielectric (assuming, of course, that it is nonmagnetic) it follows that

$$Z_0 = \frac{1}{v_0 \sqrt{CC_0}}, \tag{12}$$

where

$C_0$ is the capacity without dielectrics,
$C$ is the capacity with dielectrics present,

and that the phase velocity in the line is

$$v = v_0 \sqrt{\frac{C_0}{C}}. \tag{13}$$

It must be noted that this simple argument is not flawless. It is not difficult to see that a line having a discontinuous medium over its cross section cannot support a pure TEM wave. However, the error in assuming that it can, although frequency dependent, is usually minute, not amounting to more than a fraction of a per cent at frequencies of several Gc/s. A further discussion is given in Marcuvitz [7] and Griemsmann [8].

### D. Improving the Solution by extrapolation

Southwell [9], considering hand-relaxation methods seems the first to postulate the idea of "advancing to a finer net" in order to speed computation. In this method, the computation is commenced on a coarse net using any assumed starting solution. (The computer program starts by assuming that all interior nodes are at zero potential.) The answers thus obtained are used as a starting point for solution on a more refined net, and so on, as required. This process may be equally well employed in a digital machine with the same consequent saving of time, but more than this simple advantage results.

Based upon earlier work by Richardson [10], Culver [11] showed that the solution obtained from increasingly fine nets may be combined to extrapolate a more accurate solution. Defining the "mesh number" as the number of net widths abutting some defining dimensions, say the side $ST$, in Fig. 1, then given solutions $C_1$,

$C_2$, and $C_3$ for the capacity at mesh numbers $n_1$, $n_2$, and $n_3$ $(n_1 > n_2 > n_3)$, a better solution is

$$C = b_3 C_3 - b_2 C_2 + b_1 C_1 \tag{14}$$

where

$$b_1 = n_1{}^4(n_3{}^2 - n_2{}^2)/D$$

$$b_2 = n_2{}^4(n_3{}^2 - n_1{}^2)/D$$

$$b_3 = n_3{}^4(n_2{}^2 - n_1{}^2)/D$$

$$D = n_1{}^2 n_2{}^2(n_2{}^2 - n_1{}^2) - n_1{}^2 n_3{}^2(n_3{}^2 - n_1{}^2) + n_2{}^2 n_3{}^2(n_3{}^2 - n_2{}^2),$$

provided that the approach of these solutions to the limit is monotonic. To test monotonic convergence one computes the ratio

$$R = \frac{a_2 C_2 - a_1 C_1}{a_3 C_3} \tag{15}$$

where

$$a_1 = n_1{}^2(n_3{}^2 - n_2{}^2)$$

$$a_2 = n_2{}^2(n_3{}^2 - n_1{}^2)$$

$$a_3 = n_3{}^2(n_2{}^2 - n_1{}^2).$$

For true monotonic convergence $R$ is unity and in practice its closeness to unity gives a measure of the "goodness" of the extrapolation.

### E. Determining the Accuracy of a Numerical Solution

Having found a numerical solution, it is important to gain some idea of its accuracy. There does not, however, appear to be any purely theoretical way of doing this. The most positive way of making an estimate appears to be a numerical development of a problem having a known analytic solution, and one resembling the actual problem as closely as possible, using in each case a comparable number of nodes. Estimates of accuracy made in this way have suggested that with three- to four-thousand nodal points, errors as low as one part in $10^4$ can be obtained in computing times not exceeding two to three minutes. As far as characteristic impedance is concerned this is an order or so better than allowed by normal constructional and dielectric tolerances.

### F. Programming Aspects

It is now profitable to consider a few of the programming aspects. In the work that forms the subject of this paper it proved possible to solve problems involving up to 15 000 simultaneous equations using an IBM 7090 machine. Clearly, to use this potential to advantage, it is vital that individual problems be presented to the machine in such a way as to require a minimum of effort from the operator.

Ideally, if given a deck of data cards defining the geometry of the problem, the machine should be able to set up its own system of simultaneous equations, to solve them, to automatically advance to a finer net if so desired, to extrapolate the individual solutions, and to print out answers in a readily interpreted format. This problem of program organization proved to be more of

a test than the mathematics; however, it is a rare problem that cannot be completely solved, using no more than twenty data cards. It is not appropriate to give details here of how these data cards are written but the interested reader may consult Green [12].

After processing by the machine, in addition to the print-out of charge and capacity, the facility for print-out of the computed nodal potentials is also available on demand. This is useful when it is necessary to see whether the problem has been adequately represented by the finite difference model or where a knowledge of the field itself is desirable.

### III. A Selection of Solved Problems

The program just described was employed in the numerical solution of a large number of transmission-line problems, leading to the production of much useful data. Some of these results have been published [13], [14] but many of considerable importance will be presented in this section. Initially, attention will be given to characteristic impedance determination, but later subsections will discuss the equivalent circuits of a selection of simple obstacles.

### A. Shielded Stripline

Stripline consists basically of an inner conductor centrally placed between two plates or ground planes having a width much greater than their spacing. In a form frequently used it has an inner conductor consisting of two thin strips of copper (typically about 0.006 inch thick) formed to the desired width on each of the two faces of a supporting dielectric board that spans the width of the ground planes. In some applications, (such as directional couplers [15]) a solid rectangular inner conductor is used whereas in others, a dielectric support strip with the dielectric not protruding beyond the edges was substituted. Figure 3 shows these basic cross sections.

Various attempts have been made to obtain analytic solutions to this problem. In all cases the assumption was made that the ground planes are of infinite width and justified by the fact that the rapid exponential decay sideways of the field allows this idealized model to simulate practical cases with small error. Although this is a good approximation it is not necessary in a numerical solution, and in practical strip-line circuits it is often desired to close the ends of the cross section with metal plates.

For the strip configuration no direct analytic solution that includes the dielectric board has thus far been published [16]; two thin and unsupported strips were usually considered [17]. For the solid inner-bar configuration, Collin's variational solution [18], rather involved for numerical computation, or Getsinger's curves [19] may be used. In this section numerical solutions to these problems will be given and it will be shown that when the dielectric board extends beyond the inner conductors its neglect involves significant errors.
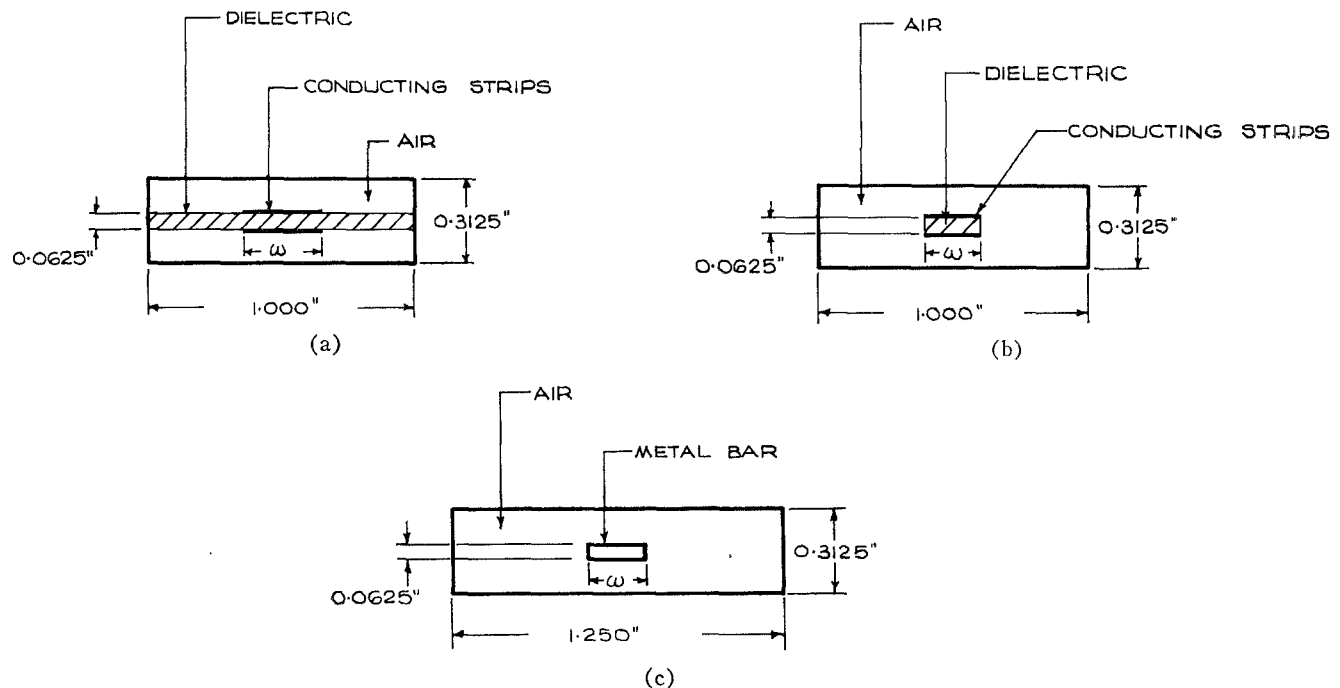
Fig. 3.   Principal forms of stripline. (a) Full dielectric support. (b) Partial dielectric support. (c) Solid inner conductor.

TABLE I

NUMERICAL DATA ON SHIELDED STRIP-LINE

| Strip Width (Inch) | Full Dielectric Support [Fig. 3(a)] | | | | | | Partial Dielectric Support [Fig. 3(b)] | | Solid Inner Bar [Fig. 3(c)] |
|---|---|---|---|---|---|---|---|---|---|
| | Teflon | | Rexolite 2200 | | Air | | Rexolite 2200 | | |
| | Char. Imp. | Vel. Rat. | Char. Imp. | Vel. Rat. | Char. Input | Vel. Rat. | Char. Input | Vel. Rat. | Char. Imp. |
| 0.1250 | | | | | | | | | 79.03 |
| 0.1563 | | | | | | | | | |
| 0.1875 | | | | | | | | | 65.27 |
| 0.2188 | 58.75 | 0.9506 | 57.38 | 0.9285 | 61.81 | 1.000 | | | |
| 0.2500 | 54.48 | 0.9540 | 53.29 | 0.9332 | 57.11 | 1.000 | | | 55.62 |
| 0.2813 | 50.79 | 0.9569 | 49.74 | 0.9372 | 53.07 | 1.000 | 53.12 | 0.9995 | |
| 0.3125 | 47.57 | 0.9594 | 46.43 | 0.9407 | 49.58 | 1.000 | | | 48.17 |
| 0.3438 | 44.72 | 0.9617 | 43.89 | 0.9348 | 46.50 | 1.000 | | | |
| 0.3750 | | | | | | | | | 42.95 |

Note:
 1. All characteristic impedances are expressed in ohms.
 2. Phase velocity ratio is given with respect to light in free space $(2.997925 \times 10^8$ m/s).

The leading dimensions of the cross sections analyzed numerically are shown in Fig. 3. Various strip widths between one-eighth inch and three-eighths inch have been examined, the principal aim being to determine the width necessary to give 50-ohms characteristic impedance and, in the case of sections containing dielectrics, to find the corresponding phase velocity. Symmetry allows treatment of a quarter of the cross section. Two dielectric constants corresponding to Teflon (2.05) and Rexolite 2200 (2.65) were used. The results obtained are summarized in Table I. Table II gives data interpolated for 50-ohm line construction.

To test the accuracy of the results, solutions were worked out from analytic formulas for two thin unsupported strips, and a solid inner bar. For the first of these check problems Cohn's [17] formula was used. This is

TABLE II

DATA FOR 50-OHM STRIP-LINE CONSTRUCTION

| Type of Line | Reference Figure | Strip Width (Inch) | Velocity Ratio |
|---|---|---|---|
| Teflon support | Fig. 3(a) | 0.289 | 0.9380 |
| Rexolite 2200 support | Fig. 3(a) | 0.279 | 0.9369 |
| Thin unsupported strips | Fig. 3(a) | 0.309 | 1.0000 |
| Solid inner bar | Fig. 3(c) | 0.298 | 1.0000 |

based on a Schwarz-Christoffel conformal transformation solution for ground planes of infinite width and involves an approximation, thought to be accurate to within 0.1 per cent for the test case $(w = 9/32$ inch) chosen, which removes one vertex from the path of integration. Cohn's formula gives a characteristic impedance of 53.40 ohms;

Fig. 4.   Slotted stripline. (a) Mechanical details. (b) Equipotential diagram.

comparison with the corresponding entry in Table I shows agreement within 0.6 per cent. As an estimate of error this will be a little pessimistic since the effect of side walls, neglected in the analytic solution, will be to slightly decrease the line impedance.

Since the error would probably not be significantly altered when the dielectric card is present, this same error would be expected in the computed impedances with both Teflon and Rexolite 2200. The error in the velocity ratio should, however, be much smaller as this involves the quotient of two nearly equal quantities having approximately the same error. For Rexolite supported line a precise experimental measurement has been made of the velocity ratio [14] which was found to agree with the computed value to within 0.3 per cent. The discrepancy can be easily accounted for by tolerances, particularly on the dielectric constant, and the neglect of the finite thickness (about 0.006 inch) of the strips.

For the solid inner bar, upper and lower bounds on the characteristic impedance were computed from Collin's [18] formulas for a bar width of 5/16 inch, and found to be 49.632 and 47.266 ohms, respectively. It will be seen that the numerical solution lies between these bounds and agrees with their mean within 0.04 per cent, a good agreement. This case was not checked experimentally.

To perform experimental work on stripline components without the need of coaxial-to-stripline transitions there is much to be said for having a slotted section available. The probe may be introduced along either of the axes of symmetry of the line; an apparatus in which it enters from the side has been described by Cohn [20]. Alternatively a slot may be cut in the center of the ground planes; this is less demanding mechanically since the probe is then inserted in a region of the field where the electric intensity vector has little or no component transverse to it. If the wall thickness of the ground plane is adequate, little slot leakage will result, but some compensation to the width of the center strip is obviously necessary if the characteristic impedance is to be maintained constant.

The slotted cross section shown in Fig. 4(a) was studied with the aid of the computer. Since the line is

no longer completely closed one of the boundary conditions to be met is that the potential at infinity is zero. While the application of numerical methods to unbounded fields will be considered in greater detail in the next section, it is satisfactory to say in the present instance that this is met with sufficient approximation by considering the slot to couple into a large conducting box straddling the slotted ground plane. Assuming Rexolite 2200 as the dielectric support material a strip width of 0.286 inch was found necessary to maintain 50 ohms characteristic impedance. This represents an increase in width of 0.007 inch over that in the absence of the slot. The corresponding velocity ratio was found to be 0.9360.

Since the field variation through the slot is clearly of some interest Fig. 4(b) shows an equipotential diagram for a slotted section having a 9/32-inch center strip. The very closely exponential decay of the field along the slot center line is most noticeable, indicating negligible leakage.

## B. Microstrip Transmission Line

In recent years a new form of TEM-mode transmission line, known as microstrip and shown in cross section in Fig. 5, has come into use [21]. Although it is mechanically very simple, mathematical analysis [22] is extremely difficult even with simplifying assumptions and most of the data available has been determined experimentally. This problem can however be handled relatively simply by numerical means.

It will be observed from Fig. 5 that this is an unbounded problem, i.e., the electric field is not confined within a finite region between the conductors, so that one of the boundary conditions which must be incorporated is that the potential at infinity is zero. The method of approximating this is by imagining the problem to be enclosed in a conducting screen of dimensions large compared with the cross section of the line. It will be noted, also, that this is a problem involving a mixed dielectric.

Figure 6 shows plots of characteristic impedance and velocity ratio for a line with a PTFE dielectric (assumed relative permittivity 2.05) and where the width of the top strip remains small compared with that of the ground plane. An analysis of the effect of the screening enclosure is given in Green [5] and for characteristic impedance the results are estimated to be in error by not more than one ohm in the range covered by Fig. 5.

## C. Steps in Coaxial Line

1) Single Steps in One Conductor Only: One of the most important applications of the program has been in the examination of the parameters of the equivalent circuits of certain simple transmission-line obstacles generated in the construction of bead supports, butt transitions, filters etc. This work has been confined to coaxial systems including, as a limiting case, parallel plate lines.
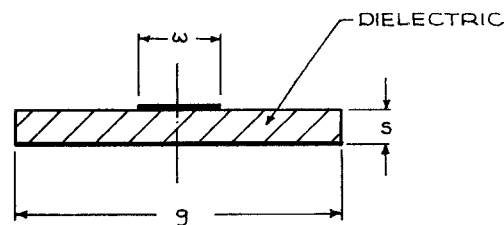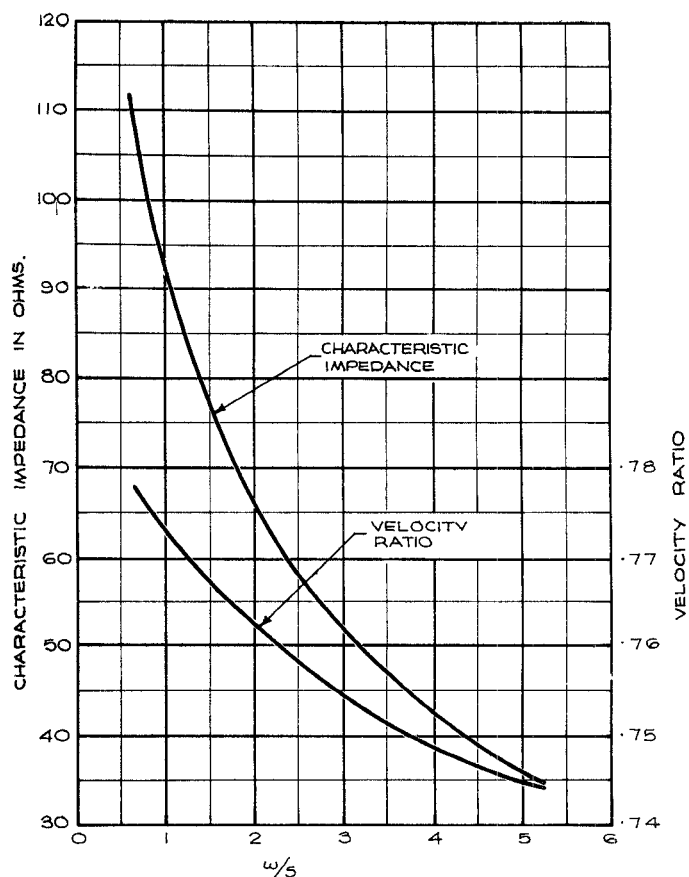


Fig. 5. Cross section of microstrip.



Fig. 6. Properties of microstrip with PTFE dielectric ($K_e = 2.05$).

One of the most commonly occurring interruptions to the longitudinal continuity of a coaxial line is the abrupt step in either the inner or outer conductor of the line (Fig. 7). It was shown by Whinnery, Jamieson, and Robbins [23] that this type of obstacle can be represented by a shunt discontinuity capacity at the plane of the step, and that this capacity is invariant with frequency if the dimensions of the line cross section remain small fractions of the wavelength of excitation. In most coaxial line applications this is the case. An analytic determination of this capacity was attempted with success.

For the parallel plate line a formula was obtained by conformal transformation [24]. For coaxial lines the conformal transformation procedure is not applicable but the problem can be attacked by the mode-matching method in which the fields on each side of the junction are expanded in an infinite series of modes matched across the boundary to preserve continuity. This was
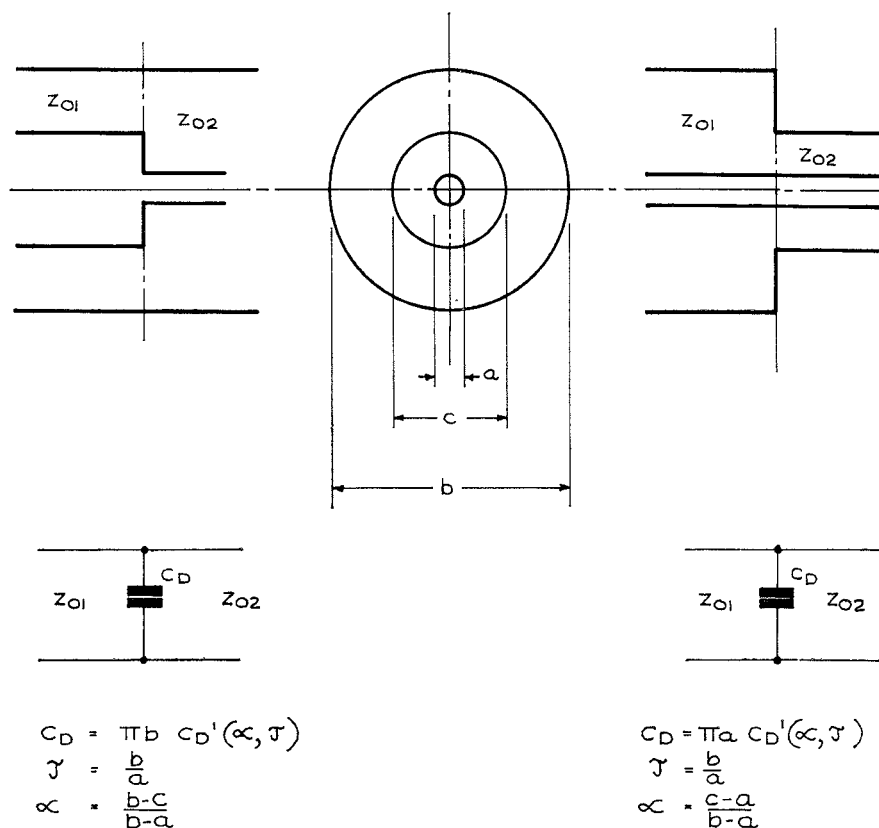
Fig. 7. Step discontinuities in coaxial lines.

TABLE III
DISCONTINUITY CAPACITY IN COAXIAL LINE

| $\alpha$ | Step in Inner Conductor | | | | | Step in Outer Conductor | | | |
|---|---|---|---|---|---|---|---|---|---|
| | $T=1$ | $T=3$ | $T=6$ | $T=11$ | $T=\infty$ | $T=1$ | $T=3$ | $T=6$ | $T=11$ |
| 0.1 | 0.10864 | 0.11072 | 0.11308 | 0.11524 | 0.13633 | 0.10864 | 0.11264 | 0.11248 | 0.13848 |
| 0.2 | 0.06977 | 0.07209 | 0.07434 | 0.07642 | 0.09630 | 0.06977 | 0.07377 | 0.08196 | 0.09503 |
| 0.3 | 0.04779 | 0.04975 | 0.05184 | 0.05379 | 0.07298 | 0.04779 | 0.05108 | 0.05763 | 0.06788 |
| 0.4 | 0.03291 | 0.03456 | 0.03643 | 0.03821 | 0.05643 | 0.03291 | 0.03545 | 0.04054 | 0.04831 |
| 0.5 | 0.02212 | 0.02344 | 0.02504 | 0.02661 | 0.04355 | 0.02212 | 0.02400 | 0.02773 | 0.03333 |
| 0.6 | 0.01408 | 0.01507 | 0.01635 | 0.01765 | 0.03298 | 0.01408 | 0.01537 | 0.01792 | 0.02168 |
| 0.7 | 0.00810 | 0.00877 | 0.00969 | 0.01069 | 0.02399 | 0.00810 | 0.00887 | 0.01064 | 0.01271 |
| 0.8 | 0.00382 | 0.00420 | 0.00475 | 0.00539 | 0.01612 | 0.00382 | 0.00418 | 0.00498 | 0.00610 |
| 0.9 | 0.00110 | 0.00123 | 0.00143 | 0.00170 | 0.00895 | 0.00110 | 0.00115 | 0.00143 | 0.00178 |
| 1.0 | 0.00000 | 0.00000 | 0.00000 | 0.00000 | 0.00000 | 0.00000 | 0.00000 | 0.00000 | 0.00000 |

Note:
Discontinuity capacities are given in pF/cm of circumference.

the approach used by Whinnery and his coworkers in 1944 and although theirs has been virtually the only data available in that time their paper suffers from two deficiencies that this new determination removes, viz.,

a) they do not consider diameter ratios beyond 5, inadequate to meet many needs, and

b) they published their answers as rather small difficult-to-read graphs. In scaling these up for publication in handbooks, often it seems by redrafting, considerable reproduction errors have occurred, causing values taken from various books to differ by several per cent.

Discontinuity capacity can be computed numerically by noting that it is equal to the difference between the total capacity of a line section including a step, and that computed by adding the contributions of two single unperturbed lines with cross-sectional dimensions and lengths equal to the actual lines on each side of the step. In setting up a model on a digital computer the observed fact that the inhomogeneous fields do not extend beyond the step that generates them by more than a diameter of the outer conductor may be used to limit the volume over which capacity must be calculated. The line may therefore be terminated by magnetic conductors one diameter each side of the step yet fully include its effects.

This problem was run on the machine to give the discontinuity capacities per unit circumferential length shown in Table III. Diameter ratios to 11 are considered.

As a guide to the accuracy of the data the discontinuity capacities obtained numerically for the limiting case of parallel plate lines were compared with the conformal transformation solutions. The agreement was found to be very good, the average correspondence being 0.4 per cent with an error exceeding one per cent only for the case where the capacity is smallest.

This method of computation can be attacked as inefficient since it demands the calculation of the total capacity to great accuracy to obtain an adequately small error in the discontinuity capacity (typically only a few percent of the total). While this is true, the computation time for the data presented in Table III averaged no more than two minutes per point.

2) *Steps in Both Conductors Simultaneously:* In some applications, such as a bead support required to restrain the inner conductor against axial displacement, it is necessary to undercut the inner conductor and overcut the outer conductor at the same reference plane to produce a doubly opening out discontinuity. A circuit representation of this double step by a single shunt capacity is still legitimate but a problem arises in determining its magnitude. Although there is no general case and any individual problem can be treated either analytically or numerically, it is obviously desirable to be able to use the data given in Table III.

Consider the discontinuity shown in Fig. 8(a). In the undisturbed field, regions $R$ and $S$ well away from the step, the lines will be radial, and the potential in the space between the inner and outer conductors will vary logarithmically with radius. There will be a certain diameter where the potentials in each of $R$ and $S$ are equal. In terms of the notation of the figure this may be determined readily as

$$r = \log^{-1} \left\{ \frac{\log a \log \dfrac{d}{c} - \log c \log \dfrac{b}{a}}{\log \dfrac{d}{c} - \log \dfrac{b}{a}} \right\} \quad (16)$$

or in the limiting case where the line has become a pair of parallel plates [Fig. 8(b)]

$$r = \frac{bc}{b + c - d} . \quad (17)$$

It is assumed that this equipotential surface will continue through the region of inhomogeneity without substantial deviation from cylindrical form. The discontinuity thus splits into two series-connected sections, each of which may be estimated from Table III.

This assumption is obviously rigorous in certain limiting cases and its general validity has been examined by comparing results obtained using it with direct numerical computations. Table IV shows typical cases. It will be seen that agreement is within ten per cent.

3) *Proximity Effects between Neighboring Discontinuities:* Often, to anchor a support bead, for example,
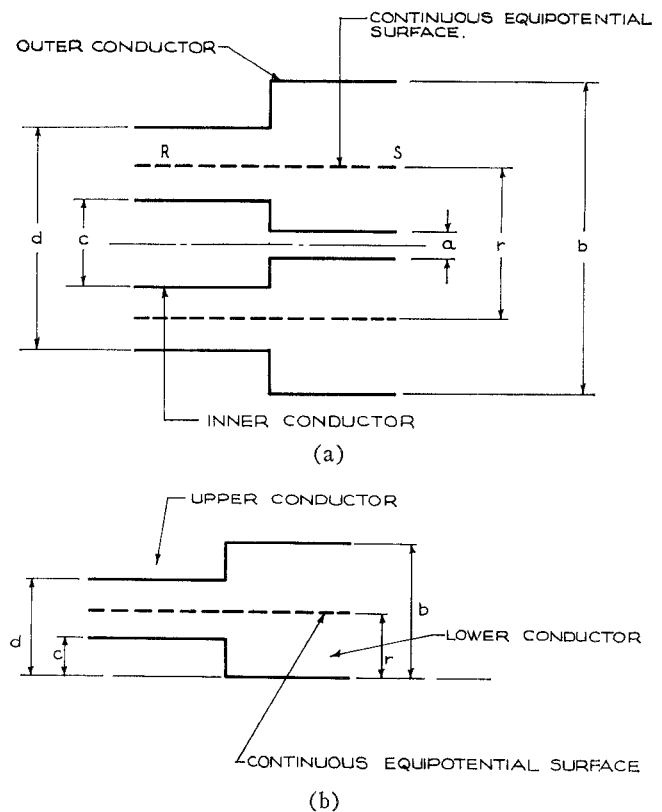


Fig. 8. Location of continuous equipotential surface through double discontinuity. (a) Double step in coaxial line. (b) Double step in parallel plate line.

TABLE IV

COMPARISON OF ACCURATE AND APPROXIMATE METHODS OF COMPUTING A DOUBLY OPENING-OUT DISCONTINUITY

| TYPE OF LINE | FIGURE | DISCONTINUITY CAPACITY (pF) | |
|---|---|---|---|
| | | ACCURATE | APPROXIMATE |
| PARALLEL PLATE |  | 0·125 | 0·111 |
| COAXIAL |  | 0 597 | 0·574 |
| COAXIAL |  | 0·298 | 0 280 |

Note:
1) Dimensions are given in centimeters.
2) For the parallel plate line, capacity is given per centimeter width normal to the section shown.
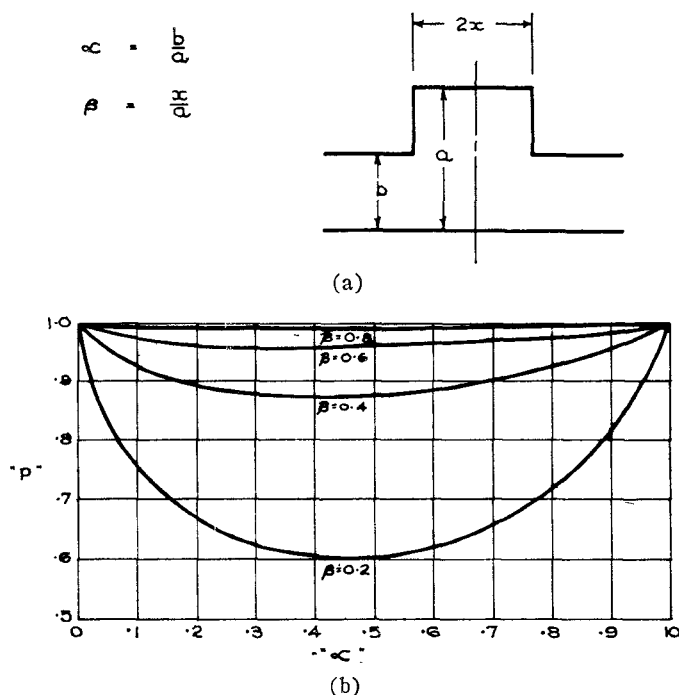
(a)

(b)

Fig. 9.    Proximity factor for double step in parallel plate line.
(a) Notation. (b) Proximity-factor curves.

TABLE V

COMPARISON OF PROXIMITY FACTOR $(P)$ FOR PARALLEL PLATE LINE
AND A "CORRESPONDING" COAXIAL LINE HAVING STEP RATIOS $(\alpha)$
OF 0.5 AND VARIOUS PROXIMITY RATIOS $(\beta)$

| Proximity Ratio | Parallel Plate Line | Coaxial Line $(T=6)$ | |
|---|---|---|---|
| | | Inner Step | Outer Step |
| 0.0 | 0.000 | 0.000 | 0.000 |
| 0.2 | 0.604 | 0.586 | 0.587 |
| 0.4 | 0.873 | 0.858 | 0.859 |
| 0.6 | 0.969 | 0.960 | 0.960 |
| 0.8 | 0.996 | 0.991 | 0.991 |
| 1.0 | 1.000 | 1.000 | 1.000 |

Note:
See Fig. 9 for notation.

(a)

(b)

(c)

Fig. 10.    Series gap in coaxial line and equivalent circuit. (a) Series gap in coaxial line. (b) Equivalent circuit of gap. (c) Circuit for analysis.

double step discontinuities, such as shown in Fig. 9(a), are created. If the distance between them is short the fringing fields generated at the steps interact in such a way as to decrease the effective discontinuity capacity at each step from the value calculated in isolation. This may be taken into account by multiplication with a proximity factor $P$.

Using the notation shown in Fig. 9, a reasonably extensive table of proximity factors has been computed for neighboring discontinuities in parallel plate line and these are shown in that figure. The error involved in applying these to discontinuities in coaxial line—where the radius of curvature of the conductors is no longer infinite—has been investigated. "Corresponding" discontinuities in parallel plate and coaxial line having a diameter ratio of 6 are compared in Table V. It is evident that there is negligible difference to the proximity factor whether the step is cut in the inner or outer con-

ductors, and that the divergence from the parallel plate case does not exceed three per cent.

D. Capacitive Gaps in Coaxial Lines

1) General Theory: A gap cut in the center conductor of a coaxial line in a plane normal to its axis finds common use in microwave band-pass filter construction where its essential purpose is to introduce series capacitive coupling. However, between the reference planes $TT'$ in Fig. 10(a) its complete representation requires the $\pi$ capacitive network shown in Fig. 10(b). For design purposes it is necessary to know both the series and shunt arms of the equivalent network. For gap and line cross-sectional dimensions which remain small compared with the wavelength, this may be treated as an electrostatic problem and may be solved as follows.

Consider the circuit shown in Fig. 10(c) in which a length of coaxial line is terminated in "half-gap," i.e., a gap bisected by the plane AA midway between the

TABLE VI

SERIES ($C_1$) AND SHUNT ($C_2$) ARMS OF EQUIVALENT NETWORK FOR GAPS IN COAXIAL LINE

| Gap Ratio | Diameter Ratio | | | | | | | | | | | | | | | |
|---|---|---|---|---|---|---|---|---|---|---|---|---|---|---|---|---|
| | 10:9 | | 4:3 | | 5:3 | | 2:1 | | 2.3:1 | | 3:1 | | 5:1 | | 7:1 | |
| | $C_1$ | $C_2$ | $C_1$ | $C_2$ | $C_1$ | $C_2$ | $C_1$ | $C_2$ | $C_1$ | $C_2$ | $C_1$ | $C_2$ | $C_1$ | $C_2$ | $C_1$ | $C_2$ |
| 0.05 | 0.367 | 0.0354 | 0.275 | 0.0143 | 0.188 | 0.00823 | 0.138 | 0.00610 | 0.109 | 0.00509 | 0.0702 | 0.00386 | 0.0316 | 0.00262 | 0.0196 | 0.00215 |
| 0.075 | 0.238 | 0.0486 | 0.183 | 0.0206 | 0.127 | 0.0120 | 0.0946 | 0.00893 | 0.0757 | 0.00746 | 0.0498 | 0.00566 | 0.0231 | 0.00382 | 0.0111 | 0.00312 |
| 0.10 | 0.173 | 0.0598 | 0.136 | 0.0265 | 0.0960 | 0.0156 | 0.0719 | 0.0116 | 0.0578 | 0.00972 | 0.0384 | 0.00737 | 0.0183 | 0.00496 | 0.00707 | 0.00402 |
| 0.15 | 0.106 | 0.0767 | 0.0858 | 0.0366 | 0.0623 | 0.0221 | 0.0474 | 0.0166 | 0.0384 | 0.0139 | 0.0259 | 0.0105 | 0.0127 | 0.00670 | 0.00822 | 0.00559 |
| 0.20 | 0.0718 | 0.0890 | 0.0598 | 0.0450 | 0.0443 | 0.0277 | 0.0340 | 0.0210 | 0.0277 | 0.0176 | 0.0188 | 0.0133 | 0.00929 | 0.00872 | 0.00606 | 0.00687 |
| 0.25 | 0.0516 | 0.0985 | 0.0436 | 0.0520 | 0.0328 | 0.0327 | 0.0254 | 0.0248 | 0.0217 | 0.0208 | 0.0143 | 0.0157 | 0.00701 | 0.0102 | 0.00461 | 0.00790 |
| 0.30 | 0.0383 | 0.106 | 0.0328 | 0.0579 | 0.0249 | 0.0369 | 0.0194 | 0.0281 | 0.0161 | 0.0235 | 0.0109 | 0.0178 | 0.00537 | 0.0113 | 0.00352 | 0.00873 |

Note:
    Entries in this table are in pF/cm of outer conductor circumference.

reference planes $TT'$. Denoting the series and shunt arms of the equivalent network of the total gap by $C_1$ and $C_2$, if a perfect short circuiting plane is inserted at AA then the line section is effectively terminated to ground through a capacity $2C_1+C_2$. If the short circuiting plane is removed to be replaced by a perfect open circuit (perfect magnetic conductor) then the line is now terminated to ground through a capacity $C_2$.

To compute these capacities the total capacity of a length of line terminated alternately as just described is calculated. To obtain valid answers the length must be sufficient to ensure that the disturbance to the normally purely radial electric field in the line has become insignificant; some preliminary numerical calculations of the potential distribution showed that a length equal to the line diameter was sufficient to ensure this. In addition, the capacity of an undisturbed section of line of this same length is determined from the usual theory. Simple arithmetic operations then suffice to deduce the equivalent circuit parameters, an extensive collection of which is given in Table VI.

*2) Comparison of the Numerical Solution with Small Aperture Theory:* Marcuvitz [25], in treating a problem related to that just given, found an approximate solution by using the small aperture technique. The geometry of this problem, consisting of a coaxial cavity closed at one end with a conducting cover plate from which the inner conductor is shorter by a gap of width $s/2$, is shown in Fig. 11(a). In reference to the plane $T$, the inner conductor is shown to be terminated to ground through a capacitance [Fig. 11(b)]

$$C = \frac{\pi a^2 \epsilon}{2s} + 2a\epsilon / \ln \frac{b-a}{s} . \qquad (18)$$

This formula is said to be valid under the restrictions

$$\lambda \gg b - a \qquad (19)$$

$$s \ll b - a \qquad (20)$$

and can be seen to consist of two distinct parts, a component giving the parallel plate capacity between the inner conductor and the cover plate and a "fringing" term.

It will be realized that $C$ is to be compared with the sum $2C_1+C_2$. Although a direct check is not possible due to the approximate nature of (18) a useful compari-
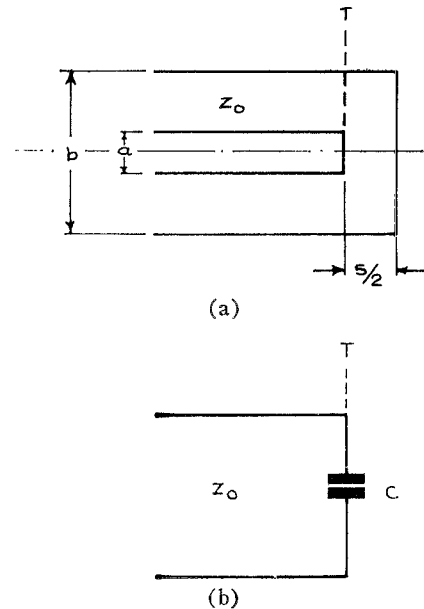


Fig. 11. Marcuvitz problem. (a) Cavity with foreshortened inner conductor. (b) Equivalent circuit.

son may be made. For the smallest gap ratio treated, agreement is within two-and-a-half percent even for the 10:9-diameter-ratio case, which clearly violates inequality (20). This and the fact that the shunt component must be zero at zero gap may be used to extend the table to smaller gap widths than those listed.

*E. Coaxial Bead Supports with Undercut Faces*

When a dielectric support bead is introduced into a coaxial line it is necessary to cut into one or both of the conducting surfaces to preserve continuity of characteristic impedance through the bead. This in itself generates a further mismatch since, as was pointed out in Section III-C, the introduction of a step into the conducting surfaces of a coaxial line is electrically equivalent to inserting a shunt capacity at the plane of the step. Various schemes were developed for the broadband compensation of the mismatch and two of the more effective ones are shown in Fig. 12. These schemes have been studied empirically in great detail by Kraus [26] but do not as yet appear to have been investigated theoretically.

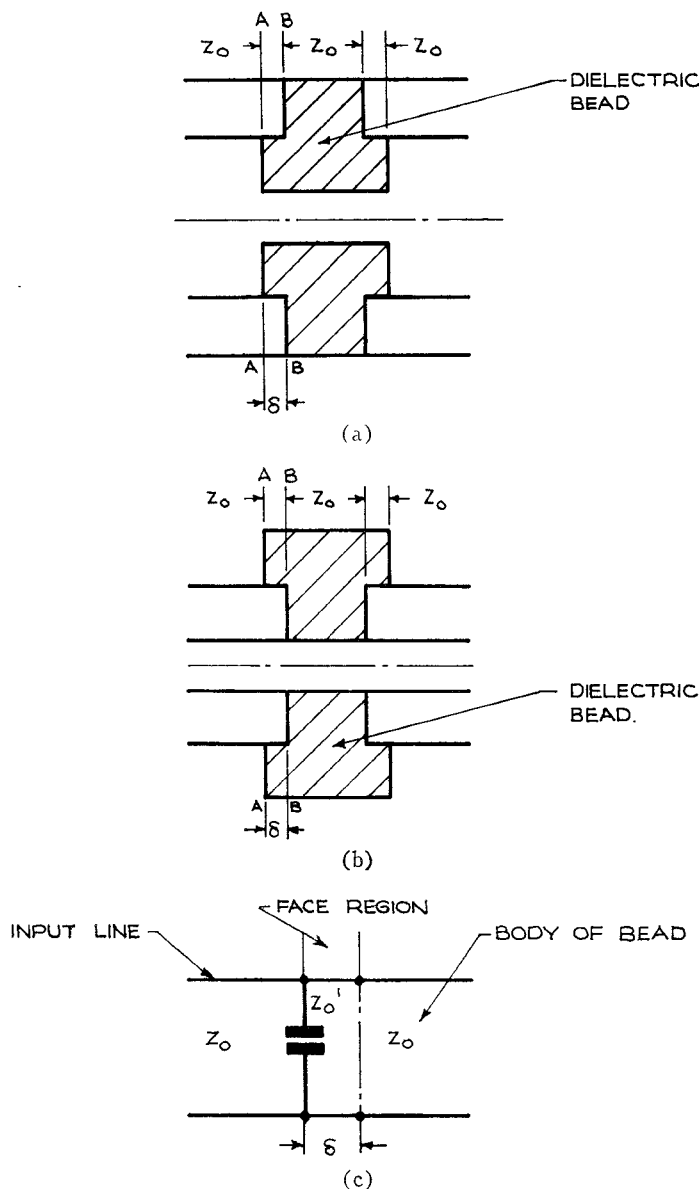It will be assumed that the beads are sufficiently long for their end regions to be considered isolated: the prob-

Fig. 12. Compensation by contouring bead face. (a) Stepped inner conductor. (b) Stepped outer conductor. (c) Equivalent circuit.

junction region (transmission line component plus discontinuity component) between $AA$ and $BB$. The zero-frequency image impedance of the junction network is, therefore,

$$Z_{i0} = \sqrt{\frac{L}{C}} \qquad (21)$$

where $L = (\delta/2\pi) \ln b/c$ is the inductance of the line between $AA$ and $BB$.

By computing $Z_{i0}$ for several values of $\delta$ it is easy to interpolate the depth which gives impedance continuity. Table VII summarizes the conditions for match in a 50-ohm line where the dielectric is Teflon ($K_e = 2.05$) and Fig. 13 shows curves of junction performance against frequency.

### F. Butt Junctions in Coaxial Lines

A common requirement in coaxial systems is a low VSWR connection between a line of one size and another of the same characteristic impedance. This requirement may arise, for example, in the connection of test equipment brought out to type "N" sockets to large rigid coaxial cable runs.

Although a taper transition may be used this is usually bulky and is relatively difficult to machine. A possible alternative is the offset butt joint shown in Fig. 14. The design requirement is to make the offset between the steps in the inner and outer conductors give sufficient inductance to compensate the excess capacity of the inhomogeneous field region.

By electrostatic means it is not possible to compute the individual discontinuity capacities occurring at each end of the junction region, but it is relatively easy to determine the total capacity of the junction. This is sufficient for design even though it is not now, as was the case with the bead support problem, possible to compute the behavior of the transition with frequency.

The butt transition has been studied experimentally by Kraus [27] who produced a series of excellent design curves for lines of 50, 60, and 75 ohms in which the dielectric medium in the transition region is air. In view of this and the large number of possible combinations of standard lines and common dielectric materials, it has not been thought practical to attempt to provide generalized data. The program may however be used to advantage in individual problems, an example of which will be given.

It was desired to construct a matched butt transition in a 50-ohm line undergoing a 2:1 step in diameter, the transition region to be filled throughout with Fluon dielectric ($K_e = 2.0$). Leading dimensions are shown in Fig. 14. Offsets increasing in steps of 0.0075 inch from 0.015 inch to 0.060 inch were tried and the image impedance of the transition computed in each case. By interpolation it was found that an offset of 0.045 inch preserves continuity of impedance. This transition was constructed experimentally by Pyle [28] who obtained

lem to be treated then is that of compensating the junction between two semi-infinite lines of equal characteristic impedance. It is assumed that the transition region may be represented by a single shunt capacitor at the plane of the step followed by a very short length of unmatched transmission line, giving the equivalent circuit shown in Fig. 12(c). The object is to determine the cutout depth $\delta$ in the dielectric so that the regions between the reference planes $AA$ and $BB$ will have a zero frequency image impedance equal to that of the adjoining transmission lines.

By terminating the lines with magnetic planes spaced about a diameter on each side of the reference planes the problem is readily handled numerically. The machine calculates the total capacity of the line and by deduction of the capacities of the terminal lines (assumed unperturbed) gives the net capacity $C$ of the

TABLE VII

DIELECTRIC BEAD COMPENSATED BY UNDERCUTTING OF BEAD FACE

| Stepped conductor | Undercut ($\delta$) (Inch) |
|---|---|
| Inner | 0.036 |
| Outer | 0.056 |

Note:
This data applies for a 50-ohm line with a maximum outer conductor diameter of one inch and a bead material of dielectric constant 2.05.
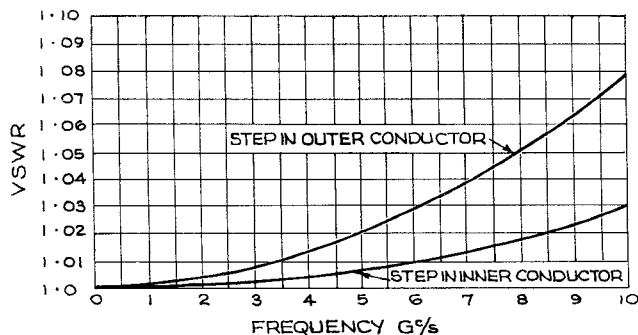


Fig. 13. Performance of beads compensated by facing-out of dielectric.
Note:
1) Maximum outer conductor diameter = 1.000 inch.
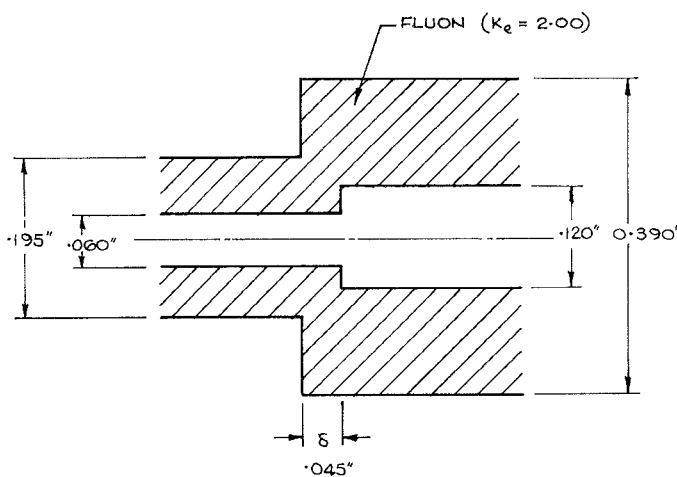2) Dielectric is Teflon ($K_e$ = 2.05).



Fig. 14. Offset but junction in coaxial lines of equal characteristic impedance.

an optimum match also at an offset of 0.045 inch; the agreement between theory and practice is, therefore, excellent.

It is of interest to note that without the dielectric filling the problem would have been equivalent to designing a matched transition in a 71-ohm line. Although Kraus [27] experimentally derived curves do not include one for this impedance it is within the range of his work, allowing a value to be interpolated. This gives an offset of 0.046 inch. This is typical of the excellent agreement that was obtained in a number of cases between Kraus' work and the numerically computed answers.

## IV. CONCLUSIONS

A technique for the solution by finite differences of two dimensional boundary value problems involving Laplace's equation was outlined and its application shown in the development of a program for the numerical analysis of these problems on a digital machine. Considerable stress was placed on generality in devising the computer program, making it possible to solve an extensive range of large problems with a minimum of effort and at great speed. Its use has been illustrated in the solution of a number of important transmission line problems, some leading to the production of considerable design data which is included in this report.

Because of its generality the program becomes an important laboratory tool which can be used as an aid in solving particular design problems as they arise. An increased precision is therefore possible in the design of transmission line components which should eliminate the need for much empirical development.

## APPENDIX A

### DEVELOPMENT OF BASIC THEORY IN A CYLINDRICAL COORDINATE SYSTEM

An outline will be given here of the development of a finite difference equation which represents Laplace's equation, written in cylindrical coordinates, for a general interior-node subject to the restriction of rotational symmetry. It will be assumed that the medium between the conducting surfaces is homogeneous and that these conducting surfaces can be drawn in by joining lines of nodes parallel to the coordinate axes, i.e., the same assumptions as those used to derive (4).

Consider the point $P$ shown in Fig. 15, a node in a net of mesh width $a$. Due to balance about the axis only half the problem need be treated. The convention is, therefore, adopted throughout this development that the first row in the net lies along the axis of symmetry. Let $P$ lie in the $N$th row (and for the present assume $N > 1$), i.e., on a radius $r = (N-1)a$. The potential at $P$ must satisfy the equation

$$\frac{\partial^2 V}{\partial r^2} + \frac{1}{r}\frac{\partial V}{\partial r} + \frac{\partial^2 V}{\partial z^2} = 0 \qquad (22)$$

which, unlike its Cartesian equivalent, involves derivatives of the first order.

Nonetheless, a Taylor expansion closely similar to that used in the main text serves to derive approximations to these derivatives in terms of the potential differences between $P$ and its four immediate neighbors. Thus

$$V_A + V_B + (1 - a/2r)V_C + (1 + a/2r)V_D - 4V_P = 0 \qquad (23)$$

is an approximation to the Laplace equation at $P$ with a dominant error

$$e = \frac{a^2}{12}\left[\frac{\partial^4 V}{\partial z^4} + \frac{\partial^4 V}{\partial r^4} + \frac{2}{r}\frac{\partial^3 V}{\partial r^3}\right], \qquad (24)$$
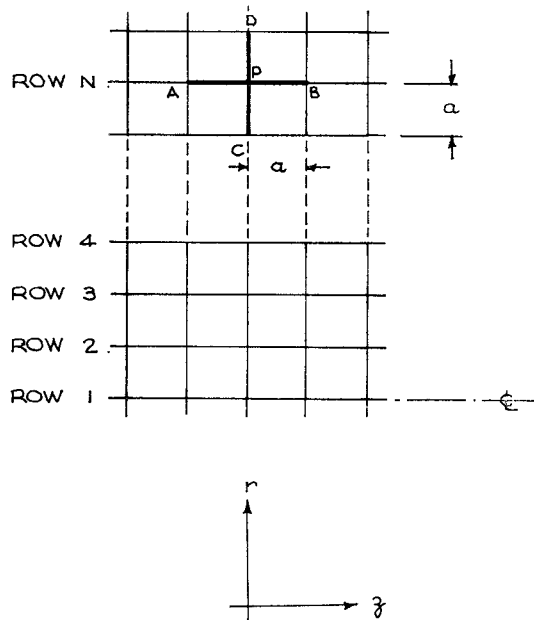
Fig. 15. Cylindrical coordinate system. Mesh representation for no variation with $\phi$.



Fig. 16. Cylindrical coordinate system point on centerline.

i.e., in the order $a^2$, as before. Equation (23) may be further simplified by substituting for the radius in terms of the position of $P$ in the net, thus

$$V_A + V_B + \frac{(2N-3)}{(2N-2)} V_C + \frac{(2N-1)}{(2N-2)} V_D - 4V_P = 0. \quad (25)$$

Special interest attaches to nodal points in row 1. As the radius is then zero and since, due to symmetry, all odd-order derivatives must be zero, the middle term of equation (22) assumes an indeterminate $(0/0)$ form in this case. Consequently, difficulty may be eliminated by reverting to the Cartesian form of the Laplace equation, for which purpose a $w$ axis is introduced to form the third of an orthogonal set with the $r$ and $z$ axes (Fig. 16). The point $P$ must then satisfy

$$\frac{\partial^2 V}{\partial r^2} + \frac{\partial^2 V}{\partial z^2} + \frac{\partial^2 V}{\partial w^2} = 0. \quad (26)$$

This is not, of course, peculiar to the axis of symmetry; any point in the space between the conductors must satisfy (26). It has not been generally applied, since, on all but the axis of symmetry, it leads to a three-dimensional net. In this one particular case, by symmetry

$$V_C = V_D = V_E = V_F,$$

and therefore expanded in finite difference form (26) leads to the two-dimensional form

$$4V_A + V_B + 4V_D - 6V_P = 0. \quad (27)$$

The calculation of charge from the potential distribution is based upon similar principles to the Cartesian case but the numerical procedures are materially altered. There is no difference in finding the normal component of displacement through the surface of integra-

tion, i.e., (8) remains valid, but the method of integration over the surface is different. Two kinds of surfaces need to be distinguished; these are surfaces of constant $r$, or cylinders about the axis of symmetry; and surfaces of constant $z$, or plane annular surfaces normal to the axis of symmetry. A given surface of integration will, in general, be generated by the interconnection of $s$ subsurfaces, some of each kind.

For a cylindrical surface in the $i$th row containing $r$ nodes

$$Q' = 2\pi(i-1)a^2\epsilon \sum_{P=1}^{r}{}' \left(\frac{\partial V}{\partial r}\right)_P. \quad (28)$$

For an annular surface in the $j$th column spanning between the $k$th and $m$th rows

$$Q' = \pi a^2\epsilon \sum_{P=1}^{m-k+1}{}' (k + P + \delta - 2)\left(\frac{\partial V}{\partial z}\right)_P. \quad (29)$$

The total charge is therefore

$$Q = \sum_s Q'. \quad (30)$$

## Appendix B

### Special Finite-Difference Equations

Both in the main text and in Appendix A, only finite-difference representation of ordinary interior nodes has been considered (with the one exception of points along the axis in a cylindrical system). Most nodes will fall into this category but to take account of all possible boundary conditions there are 28 other possible conditions which may arise.

Having read in details of conductor boundaries and the disposition of dielectrics the machine is made to scan the net, node by node, to identify whether they

are ordinary interior points or one of the exceptional cases. If found to be the latter, the node number is recorded in an "oddity table" (generated automatically by the machine) together with a further identification number. According to the convention indicated in Table VIII, these criteria indicate in what way the node is exceptional.

When the equations of the potentials are being solved the machine first determines whether that node was included in the oddity table. If it was not, the point is relaxed according to the standard equation for an ordinary interior node; if the node was included, the machine is directed to a special equation appropriate to the kind of oddity. The finite difference equations for each of the 28 types of oddity are listed in Table VIII for both Cartesian and cylindrical systems. Since each of these equations may be derived by application of Taylor's theorem, individual proofs will not be given.

### ACKNOWLEDGMENT

TABLE VIII

SPECIAL FINITE DIFFERENCE EQUATIONS

| ODDITY Nº | DESCRIPTION | | | FIGURE | CARTESIAN EQUATION | CYLINDRICAL EQUATION |
|---|---|---|---|---|---|---|
| 1 | ORDINARY INTERIOR POINT | | | | SEE TEXT, EQUATION (4) | SEE APPENDIX I, EQUATION (30) |
| 2 | ORDINARY POINT | | BOTTOM EDGE | | $V_A + V_B + 2V_D - 4V_P = 0$ | SEE APPENDIX I, EQUATION (32) |
| 3 | | | TOP-EDGE | | SIMPLE PERMUTATION OF (2) | $V_A + V_B + 2V_C - 4V_P = 0$ |
| 4 | | | LEFT-HAND EDGE | | SIMPLE PERMUTATION OF (2) | $4(N-1)V_B + (2N-3)V_C + (2N-1)V_D - 8(N-1)V_P = 0$ |
| 5 | | | RIGHT-HAND EDGE | | SIMPLE PERMUTATION OF (2) | SIMPLE PERMUTATION OF (4) |
| 6 | CORNER POINT | BOTTOM | LEFT-HAND SIDE | | $V_B + V_D - 2V_P = 0$ | $V_B + 2V_D - 3V_P = 0$ |
| 7 | | | RIGHT-HAND SIDE | | SIMPLE PERMUTATION OF (6) | SIMPLE PERMUTATION OF (6) |
| 8 | | TOP | LEFT-HAND SIDE | | SIMPLE PERMUTATION OF (6) | $V_B + V_C - 2V_P = 0$ |
| 9 | | | RIGHT-HAND SIDE | | SIMPLE PERMUTATION OF (6) | SIMPLE PERMUTATION OF (8) |
| 10 | DIELECTRIC INTERFACE | ROW INTERFACE | DIELECTRIC TO TOP | | $(1+K_e)V_A + (1+K_e)V_B + 2V_C + 2K_e V_D - 4(1+K_e)V_P = 0$ | $\{2N(K_e+1)-(K_e+3)\}V_A + \{2N(K_e+1)-(K_e+3)\}V_B + 2(2N-3)V_C + 2K_e(2N-1)V_D - 4\{2N(K_e+1)-(K_e+3)\}V_P$ |
| 11 | | | DIELECTRIC TO BOTTOM | | SIMPLE PERMUTATION OF (10) | $\{2N(K_e+1)-(3K_e+1)\}V_A + \{2N(K_e+1)-(3K_e+1)\}V_B + 2K_e(2N-3)V_C + 2(2N-1)V_D - 4\{2N(K_e+1)-(3K_e+1)\}V_P = 0$ |
| 12 | | COLUMN INTERFACE | DIELECTRIC TO LEFT-HAND SIDE | | SIMPLE PERMUTATION OF (10) | $4K_e(N-1)V_A + 4(N-1)V_B + (2N-3)(K_e+1)V_C + (2N-1)(K_e+1)V_D - 8(N-1)(K_e+1)V_P = 0$ |
| 13 | | | DIELECTRIC TO RIGHT-HAND SIDE | | SIMPLE PERMUTATION OF (10) | SIMPLE PERMUTATION OF (12) |
| 14 | ANGLE DIELECTRIC | ACUTE | FIRST QUADRANT | | $2V_A + (K_e+1)V_B + 2V_C + (K_e+1)V_D - 2(K_e+3)V_P = 0$ | $4(N-1)V_A + \{2N(K_e+1)-(K_e+3)\}V_B + 2(2N-3)V_C + (2N-1)(K_e+1)V_D - 2\{2N(K_e+3)-(K_e+7)\}V_P = 0$ |
| 15 | | | SECOND QUADRANT | | SIMPLE PERMUTATION OF (14) | SIMPLE PERMUTATION OF (14) |
| 16 | | | THIRD QUADRANT | | SIMPLE PERMUTATION OF (14) | $\{2N(K_e+1)-(3K_e+1)\}V_A + 4(N-1)V_B + (2N-3)(K_e+1)V_C + 2(2N-1)V_D - 2\{2N(K_e+3)-(3K_e+5)\}V_P = 0$ |
| 17 | | | FOURTH QUADRANT | | SIMPLE PERMUTATION OF (14) | SIMPLE PERMUTATION OF (16) |
| 18 | | OBTUSE | FIRST QUADRANT | | $2K_e V_A + (K_e+1)V_B + 2K_e V_C + (K_e+1)V_D - 2(3K_e+1)V_P = 0$ | $4(N-1)V_A + \{2N(K_e+1)-(K_e+3)\}V_B + 2(2N-3)V_C + (2N-1)(K_e+1)V_D - 4(N-1)(3K_e+1)V_P = 0$ |
| 19 | | | SECOND QUADRANT | | SIMPLE PERMUTATION OF (18) | SIMPLE PERMUTATION OF (18) |
| 20 | | | THIRD QUADRANT | | SIMPLE PERMUTATION OF (18) | $\{2N(K_e+1)-(K_e+3)\}V_A + 4(N-1)V_B + (2N-3)(K_e+1)V_C + 2(2N-1)V_D - 4(K_e+3)(N-1)V_P = 0$ |
| 21 | | | FOURTH QUADRANT | | SIMPLE PERMUTATION OF (18) | SIMPLE PERMUTATION OF (20) |

Table VIII (*contin'd*)

| ODDITY N | DESCRIPTION | | | FIGURE | CARTESIAN EQUATION | CYLINDRICAL EQUATION |
|---|---|---|---|---|---|---|
| 22 | DIELECTRIC INTERFACE TO- | BOTTOM EDGE | DIELECTRIC TO LEFT-HAND SIDE | | $K_e V_A + V_B + (K_e+1)V_D + 2(K_e+1)V_p = 0$ | $K_e V_A + V_B + 2(K_e+1)V_D - 3(K_e+1)V_p = 0$ |
| 23 | | | DIELECTRIC TO RIGHT-HAND SIDE | | SIMPLE PERMUTATION OF (22) | SIMPLE PERMUTATION OF (22) |
| 24 | | TOP EDGE | DIELECTRIC TO LEFT-HAND SIDE | | SIMPLE PERMUTATION OF (22) | $(2N-3)K_e V_A + (2N-3) V_B + (2N-3)(K_e+1)V_C$ $-2(2N-3)(K_e+1)V_p = 0$ |
| 25 | | | DIELECTRIC TO RIGHT-HAND SIDE | | SIMPLE PERMUTATION OF (22) | SIMPLE PERMUTATION OF (24) |
| 26 | | LEFT-HAND EDGE | DIELECTRIC TO TOP | | SIMPLE PERMUTATION OF (22) | $\{2N(K_e+1)-(K_e+3)\}V_B + (2N-3) V_C + (2N-1) K_e V_D$ $-2\{2N(K_e+1)-(K_e+3)\}V_p = 0$ |
| 27 | | | DIELECTRIC TO BOTTOM | | SIMPLE PERMUTATION OF (22) | $\{2N(K_e+1)-(3K_e+1)\}V_B + (2N-3)K_e V_C + (2N-1)V_D$ $-2\{2N(K_e+1)-(3K_e+1)\}V_p = 0$ |
| 28 | | RIGHT-HAND EDGE | DIELECTRIC TO TOP | | SIMPLE PERMUTATION OF (22) | SIMPLE PERMUTATION OF (26) |
| 29 | | | DIELECTRIC TO BOTTOM | | SIMPLE PERMUTATION OF (22) | SIMPLE PERMUTATION OF (27) |

the development of the program. For reasons of speed, some of the more frequently repeated subroutines were coded in FAP; these were written in their entirety by B. P. McDowall. He also contributed many useful ideas throughout the remainder of the work and it is in no small measure due to his efforts that the project was brought to successful conclusion.

The author also wishes to thank C. T. Carson for making it possible to undertake this work and the Chief Scientist of the Department of Supply for permission to publish it.

## REFERENCES

[1] D. W. Martin and G. J. Tee, "Iterative methods for linear equations with a symmetric positive definite matrix," *Computer J.*, vol. 4, pp. 242–254, October 1961.
[2] G. A. Korn and T. M. Korn, *Mathematical Handbook for Scientists and Engineers*, 1st ed. New York: McGraw-Hill, 1961, sect. 3.2, ch. 20, p. 637.
[3] S. P. Franckel, "Convergence rates of iterative treatments of partial differential equations," *M.T.A.C.*, vol. 4, pp. 64–75, 1950.
[4] B. A. Carré, "The determination of the optimum accelerating factor for successive over relaxation," *Computer J.*, vol. 4, pp. 73–78, 1961.
[5] H. E. Green, "An extension of the results obtained by the application of the numerical solution of Laplace's equation to transmission line problems," Weapons Research Establishment, Salisbury. South Australia., Tech. Note PAD 98, December 1964.
[6] H. J. Reich, et al., *Microwave Theory and Techniques*, 1st ed. New York: Van Nostrand, 1953, sect. 1.3, ch. 1, p. 35.
[7] N. Marcuvitz, *Waveguide Handbook*, no. 10, Mass. Inst. Tech. Rad. Lab. Ser., 1st ed. New York: McGraw-Hill, 1951, sect. 4, ch. 8, p. 396.
[8] J. W. E. Griesmsmann, "Handbook of data on cable connectors for microwave use," U. S. Dept. of Navy, Bur. of Ships, Doc. Navships 900, 136A, sect. 2, ch. 2, pp. 23–28.
[9] R. V. Southwell, *Relaxation Methods in Theoretical Physics*, 1st ed. Oxford, England: Clarendon, 1946.
[10] L. F. Richardson, *Phil. Trans. Roy. Soc (London)*, pt. A, p. 307, 1911.
[11] R. C. Culver, "The use of extrapolation techniques with electrical network analogue solutions," *Brit. J. Appl. Phys.*, vol. 3, pp. 376–378, December 1952.
[12] H. E. Green, "The numerical calculation of the characteristic

impedance, propagation constant and the equivalent circuits of obstacles in TEM mode transmission lines," Weapons, Research Establishment, Salisbury, South Australia, Rept. PAD 14, July 1964.
[13] H. E. Green, "The characteristic impedance of square coaxial line," *IEEE Trans. on Microwave Theory and Techniques (Correspondence)*, vol. MTT-11, pp. 554–555, November 1963.
[14] H. E. Green and J. R. Pyle, "The characteristic impedance and velocity ratio of dielectric-supported stripline," *IEEE Trans. on Microwave Theory and Techniques (Correspondence)*, vol. MTT-13, pp. 135–137, January 1965.
[15] E. M. T. Jones and J. T. Bolljahn, "Coupled-strip-transmission-line filters and directional couplers," *IRE Trans. on Microwave Theory and Techniques*, vol. MTT-4, pp. 75–81, April 1956.
[16] K. Foster, "The characteristic impedance and phase velocity of high Q triplate line," *J. Brit. IRE*, vol. 8, pp. 715–723, December 1958.
[17] S. B. Cohn, "Characteristic impedances of broadside-coupled strip transmission lines," *IRE Trans. on Microwave Theory and Techniques*, vol. MTT-8, pp. 633–637, November 1960.
[18] R. E. Collin, *Field Theory of Guided Waves*, 1st ed. New York: McGraw-Hill, 1956, sect. 5, ch. 4, pp. 155–164.
[19] W. J. Getsinger, "Coupled rectangular bars between parallel plates," *IEEE Trans. on Microwave Theory and Techniques*, vol. MTT-10, pp. 65–72, January 1962.
[20] S. B. Cohn, "Problems in strip transmission lines," *IRE Trans. on Microwave Theory and Techniques*, vol. MTT-3, pp. 119–126, March 1955.
[21] D. D. Grieg and H. F. Engelmann, "Microstrip—A new transmission line technique for the kilomegacycle range," *Proc. IRE*, vol. 40, pp. 1644–1650, December 1952.
[22] K. G. Black and T. J. Higgins, "Rigorous determination of the parameters of microstrip transmission lines," *IRE Trans. on Microwave Theory and Techniques*, vol. MTT-3, pp. 93–113, March 1955.
[23] J. R. Whinnery, H. W. Jamieson, and T. E. Robbins, "Coaxial-Line Discontinuities," *Proc. IRE*, vol. 32, pp. 695–709, November 1944.
[24] M. Walker, *Conjugate Functions for Engineers*, 1st ed. London: Oxford U.P., 1933, pp. 53–65.
[25] N. Marcuvitz, *Waveguide Handbook*, 1st ed. New York: McGraw-Hill, 1951, sect. 5, ch. 4, p. 178.
[26] A. Kraus, "Mess kurven des Reflexions-Koeffizienten Kompensierter Inhomogenitaten bei Koaxialen Leitungen und die daraus ermittelte optimale Dimensionierung," *Rhode and Schwarz Mitteilungen (Germany)*, No. 14, 1960.
[27] —— Mess kurven des Reflexions-Koeffizienten Kompensierter Inhomogenitaten bei Koaxialen Leitungen und die daraus ermittelte optimale Dimensionierung," *Rhode and Schwarz Mitteilungen, (Germany)*, No. 8, 1956.
[28] J. R. Pyle, private communication.